Analyst

PAPER

View Article Online
View Journal | View Issue

Cite this: *Analyst*, 2018, **143**, 5023

Analysis of human menisci degeneration *via* infrared attenuated total reflection spectroscopy†

Pei Wang,[a] Jonas Balko,[b] Rui Lu,[c] Ángela I. López-Lorente,[d] Lutz Dürselen[b] and Boris Mizaikoff*[a]

Degeneration of human meniscal tissue induces impairment of normal knee functions, and is a highly relevant etiology of knee joint tears and osteoarthritis. Currently, the grading scale of meniscus degeneration is conventionally derived from evaluating meniscal morphology and histological staining. However, mid-infrared attenuated total reflectance (IR-ATR) spectroscopy is a particularly useful technique that may analyze the biomolecular composition at a sample surface, and provide information on the intra- and/or inter-molecular chemical bonds. In the present study, 61 lyophilized human menisci samples at different grades of degeneration were analyzed *via* IR-ATR spectroscopy in a label-free fashion, and the data were evaluated *via* Gaussian peak fitting and 2D correlation analysis. During increasing meniscal degeneration (*i.e.*, grade 1 to 4) along with calcification at grade 4, an evident blue shift of the amide I band (1700–1600 cm^{-1}) was observed in the associated IR spectra. In addition, Gaussian peak fitting revealed significant area variance of the fitted sub-peaks. 2D correlation spectra provided further access to detailed changes of the amide I band during the degeneration process. Derived from this multi-tiered data analysis taking into account the protein secondary structure information within the amide I band, and the triple helical structure of meniscal collagen, the blue shift and peak area changes during meniscus degeneration are indicative of collagen fibril formation during evolving degeneration. Furthermore, a degradation of the water-binding proteoglycan and collagen network especially for degenerated menisci with calcification was observed. Results were compared with a collagen–chondroitin sulphate mixture model, confirming the observed changes in collagen fibrils and proteoglycans. In summary, this study confirms the utility of IR-ATR spectroscopy as a versatile tool providing access to meniscal tissue degeneration processes at molecular level detail, and may in future evolve into a useful diagnostic instrument for analyzing cartilage degeneration.

Received 18th May 2018,
Accepted 2nd September 2018

DOI: 10.1039/c8an00924d

rsc.li/analyst

Introduction

Human menisci are semilunar formed and fibrocartilaginous tissues, which are located between the femoral condyles and the tibial plateau.[1] Menisci serve a variety of complex biomechanical functions including load transmission across the knee, shock absorption, joint stabilization and lubrication, articular cartilage protection, and nutrition.[1–3] Degeneration of meniscal tissue induces an impairment of these functions, and acts as a highly relevant indicator of knee joint tears and osteoarthritis (OA).[4] During aging or osteoarthritic processes, macroscopic and microscopic changes can be distinctly observed in human menisci. In 2011, Pauli *et al.* developed an advanced grading system for scoring the degree of meniscus degeneration *via* evaluating meniscus morphology and sectional histological staining, which reveals the major microscopic differences of degraded meniscus in cellularity distribution, collagen fiber organization, and extracellular matrix.[5]

The mechanical properties of menisci are determined by its biomolecular composition and microstructural arrangement. Meniscal tissue is highly hydrated containing approx. 72% water by wet weight. The remaining mass is comprised of organic matter, *i.e.*, mostly collagens (75% of dry weight), and glucosaminoglycans (GAGs; 17% of dry weight).[1] In each region of the meniscal tissue, different types of collagen are present at varying quantities,[6] and are organized in three

[a]*Institute of Analytical and Bioanalytical Chemistry, Ulm University, 89081 Ulm, Germany. E-mail: boris.mizaikoff@uni-ulm.de*
[b]*Institute of Orthopaedic Research and Biomechanics, Trauma Research Center, Ulm University-Medical Center, 89081 Ulm, Germany*
[c]*Jiangsu Key Laboratory of Chemical Pollution Control and Resources Reuse, School of Environmental and Biological Engineering, Nanjing University of Science and Technology, 210094 Nanjing, China*
[d]*Departamento de Química Analítica, Instituto Universitario de Investigación en Química Fina y Nanoquímica IUIQFN, Universidad de Córdoba, Campus de Rabanales, E-14071 Córdoba, Spain*

†Electronic supplementary information (ESI) available. See DOI: 10.1039/c8an00924d

distinct layers in cross-section.[7] This biomolecular composition changes during degeneration processes.[8] Currently, the grading scale of meniscus degeneration is derived from conventional histological staining, while other techniques find less routine usage such as immunohistochemical markers[9] or label-free methods including infrared spectroscopy.[10,11]

Infrared attenuated total reflectance (IR-ATR) spectroscopy techniques are particularly suitable for studying biomolecular composition and structure at a sample surface in a label-free fashion. Molecular characteristics are provided *via* the analysis of vibrational bands associated with intra- and/or inter-molecular chemical bonds. For example, within the IR spectrum of a protein, the amide I band (1600–1700 cm^{-1}) primarily results from the C=O stretching vibrations, while the amide II band (1500–1600 cm^{-1}) arises predominantly from N–H bending and C–N stretching vibrations of the peptide backbone.[12–14] Due to different hydrogen-bonding environments within α-helix, β-sheet, β-turn or random structures, the amide I band is especially sensitive to the secondary structure of proteins.[12,14,15] Likewise, seminal studies have shown that IR spectroscopy and related techniques can reveal the distribution of different types of collagen in tissues, and may differentiate normal and degenerative cartilaginous material.[16–18]

The aim of the present study was the detailed analysis of human menisci samples at different stages of degeneration *via* label-free IR-ATR spectroscopy in combination with advanced data evaluation strategies. It is a first step towards the elucidation of the changes observed in the IR spectra within tissue degeneration. The amide I band of human meniscus IR spectra were fitted by Gaussian peaks, and compared between different degradation grades for alignment with the changes described by Pauli's scoring system. Furthermore, two-dimensional (2D) correlation analysis was executed for further detailing molecular and structural change within the associated IR spectra at increasing degrees of degeneration. A collagen–chondroitin sulphate mixture model was used to compare and confirm the observed changes in the spectra related to collagen fibrils and proteoglycans. Last but not least, this study lays the foundation for future *in vivo* applications of miniaturized IR-ATR catheter systems enabling label-free direct diagnosis of cartilage damage during arthroscopic procedures.

Experimental

Human menisci samples

Human menisci segments were supplied by the Institute of Orthopaedic Research and Biomechanics at Ulm University. Lateral menisci were taken from 24 patients of the University and Rehabilitation Hospital Ulm (16 women, 8 men, age: 67.1 ± 9.0 years, BMI: 29 ± 5 kg m^{-2}), who underwent total knee replacement due to radiologically significant (Kellgren and Lawrence: 1 × grade 2, 8 × grade 3 and 15 × grade 4) and clinically relevant osteoarthritis. IRB approval for taking samples from the patients was obtained (approval number 70/16).

Cylindrical menisci samples had a diameter of 4.6 mm, and were collected at the inner meniscal circumference from various sections of human menisci[19] by arthroscopy according to the Seitz protocol.[20] Initially, the degeneration grade of each sample was determined based on Pauli's scoring system *via* analyzing meniscus morphology and sectional histological staining (see Fig. S1, ESI†). In addition, three-staged confined-compression-relaxation tests were executed for calculating the aggregate modulus and permeability according to the Seitz protocol.[20] After these routine tests, the samples were lyophilized and stored at room temperature.

Prior to IR-ATR studies, the samples were smoothed at both sides using sand paper (1200/2400), and cleaned under strong nitrogen blow such that a uniform pressure could be achieved across the sample cross-section when located at the ATR crystal surface.

IR-ATR measurements

The IR-ATR spectra of human menisci samples were recorded *via* a Bruker Alpha FT-IR spectrometer (Bruker Optik Gmbh, Ettlingen, Germany) equipped with a single-reflection ATR module using a diamond ATR crystal and a pressure applicator (Platinum ATR, Bruker Optik Gmbh, Ettlingen, Germany).

Each sample spectrum represents an average of 500 spectral scans recorded at a spectral resolution of 2 cm^{-1} in the range of 4000–800 cm^{-1}. To ensure the reproducibility of the experiments, average spectra were calculated after repeating three independent measurements for each sample. Background spectra were recorded at identical conditions using the neat diamond waveguide as reference. Fig. S2 (ESI†) shows an example of the full IR-ATR spectra of a meniscus sample with grade 3 degeneration.

Data processing and spectra analysis

During IR data processing, spectral interferences by water vapour and CO_2 were efficiently excluded using automated data evaluation routines provided by the OPUS 6.5 software package (Bruker Optik Gmbh, Ettlingen, Germany). Thereafter, all spectra were smoothed using a 13-point Savitzky–Golay filter.

After selecting the spectral regime of the amide I band (namely 4000–3800 cm^{-1} and 1820–1780 cm^{-1}), the MATLAB R2013b software package (The MathWorks, Natick, MA, USA) was utilized to correct the baseline of each selected spectrum peak by start-end points and normalization of the amide I band to an area of one.

In addition, the amide I band of each meniscus sample was analyzed by using second derivatives and a Gaussian peak-fit model using the PeakFit software package (Systat Software Inc., San Jose, California). The sub-peak center wavenumber of the fitted bands were restricted to 10 cm^{-1} wavenumbers enabling the evaluation and comparison of the area changes of individual components (*i.e.*, secondary structure elements) within one band. The data obtained by comparison of the sub-peak area percentages was statistically validated by *F*-tests and *T*-tests using Excel (Microsoft, USA).

2D correlation spectroscopy

Two-dimensional (2D) correlation spectroscopy in the infrared regime was initially developed by Noda,[21] who introduced and applied perturbation-based 2D spectroscopy in this electromagnetic window. The synchronous and asynchronous correlation spectra represent the two orthogonal components within 2D correlation spectroscopy. The synchronous correlation spectrum illustrates the intensity changes in the original dataset, and the direction of the change. The asynchronous correlation spectrum provides information on the event sequence, if the external perturbation is time. All 2D correlation spectra were calculated from the normalized amide I bands of differently degraded cartilage samples using the software package 2Dshige (© Shigeaki Morita, Kwansei-Gakuin University, 2004–2005).

Mixture model of chondroitin sulphate and collagen

Chondroitin sulphate sodium salt from bovine cartilage (C6737) and collagen from calf skin (C9791) were purchased from Sigma-Aldrich Co. (St Louis, MO), and used without further purification. Both were weighted and mixed using a mill system (MM 400, Retsch, Germany) at the ratios given in Table 1. Each ratio was analysed using the same IR-ATR procedure later applied for the human menisci with exception the number of spectral scan set at 100. The average of three measurements were calculated for each mixture.

Results

Blue shift of the amide I band with increasing degeneration

The IR-ATR spectra reflect molecule vibrational patterns, which represent the molecular composition and structure of the investigated human menisci. For all samples, the spectral region of amide I band (1700–1590 cm^{-1}) was selected, baseline corrected, and the area normalized. Fig. 1 shows averaged IR-ATR spectra representative for different grades of cartilage degradation.

Besides the conventional four degeneration grades, the samples at a score of grade 4 score with accompanying calcification were treated as a separate fifth group, as their amide I band was apparently distinctly affected.

As shown in Fig. 1, an obvious blue shift and slight change of the amide I peak shape illustrates a gradual spectral change associated with the degree of degeneration. Comparing the 5 groups of degradation, the peak maximum of amide I band shifts from 1635 cm^{-1} (grade 1) to 1639 cm^{-1} (grade 4 with calcification). Moreover, the absorbance in the region around 1630 cm^{-1} wavenumber decreases, whereas the region around 1660 cm^{-1} wavenumber increases with increasing degeneration.

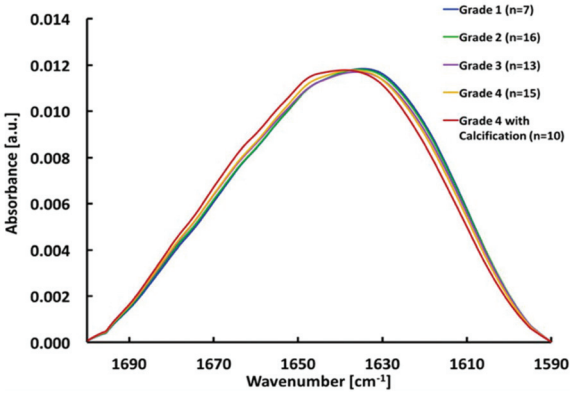

Fig. 1 Averaged IR-ATR spectra of human menisci samples at different degree of degeneration following the grade 1–4 nomenclature. Grade 4 samples with calcification were treated as a separate group.

Variance of the sub-peaks area with increasing degeneration

Different hydrogen-bonding environments within the secondary structure of proteins absorb at different wavenumber regimes, *i.e.*, α-(like) helices (1658 cm^{-1}), β-sheets (1679 and 1626 cm^{-1}), β-turns (1691 and 1669 cm^{-1}), triple helices (1637 cm^{-1}), side chains (1608 cm^{-1}), and random structures (1647 cm^{-1}).[14,15,17]

Hence, the amide I band of the investigated human menisci samples were appropriately deconvoluted and fitted with Gaussian sub-peaks, as previously described.

All Gaussian-peak-fitted amide I bands were deconvoluted with a coefficient of determination of $r^2 > 0.999$. Furthermore, the area percentage of the sub-peaks was calculated, and is shown in Fig. 2. As proved by *F*-tests and *T*-tests, the main differences between the groups are predominantly associated with the shoulder sides of the amide I band. The area percentages at the lower wavenumber region are of decreasing tendency, while the area percentages at the higher wavenumber region are increasing during progress of the degeneration. Especially, the 1660 cm^{-1} sub-peak reveals significant differences between grade 1, grade 4, and grade 4 with calcification. In addition, the 1620 cm^{-1} sub-peak shows a significant difference between grade 1 and grade 4, as well as grade 1 and grade 4 with calcification.

2D correlation spectra revealing changes in protein secondary structure during degeneration

In 2D correlation spectra, the synchronous intensity $\Phi(\upsilon 1, \upsilon 2)$ illustrates consistent trends in between separate intensity vari-

Table 1 Weight percentage (%) of collagen within the prepared collagen/chondroitin sulphate mixtures

Collagen	Set point	95	90	85	80	75	70	65	60
	Actual value	96	94.3	84.4	81	75.7	70.4	65.1	58.8

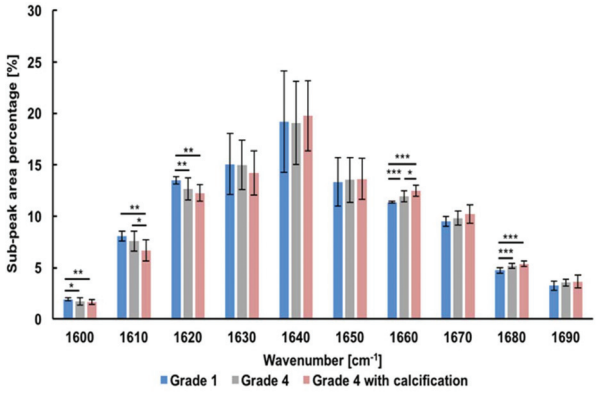

Fig. 2 Area percentage of the sub-peaks within the deconvoluted amide I bands shown for grade 1, n = 7; grade 4, n = 15; and grade 4 with calcification, n = 10.

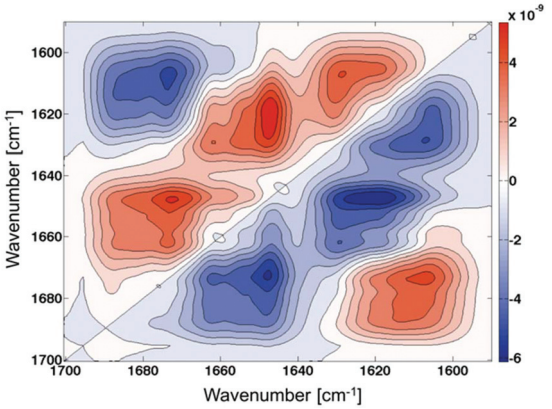

Fig. 4 Asynchronous 2D correlation spectrum of human menisci during progressing degeneration.

ations. The asynchronous intensity $\Psi(\upsilon1, \upsilon2)$ represents the dissimilarity of the spectral intensity variations. Based on Noda's rules with time as the external perturbation, if $\Phi(\upsilon1, \upsilon2) > 0$, $\Psi(\upsilon1, \upsilon2) > 0$ or $\Phi(\upsilon1, \upsilon2) < 0$, $\Psi(\upsilon1, \upsilon2) < 0$, the $\upsilon1$ intensity changes earlier in order of occurrence compared to $\upsilon2$. However, if $\Phi(\upsilon1, \upsilon2) < 0$, $\Psi(\upsilon1, \upsilon2) > 0$ or $\Phi(\upsilon1, \upsilon2) > 0$, $\Psi(\upsilon1, \upsilon2) < 0$, the sequential order of occurrence would reverse.[21]

The peak shape change of the normalized amide I band is revealed in detail *via* the synchronous 2D correlation spectrum shown in Fig. 3. There are two auto-peaks with their maximum at 1617 cm^{-1} and 1664 cm^{-1}, respectively. Both auto-peaks cover a region of approx. 40 cm^{-1}, which indicates the degeneration process occurs for a wide range of involved biomolecules. In the two auto-peaks, the one at 1617 cm^{-1} has a higher value, which illustrates that the change in the 1617 cm^{-1} region is more pronounced compared to any other region. Furthermore, as represented by the cross-peaks, the change in direction of the 1617 cm^{-1} region is decreased and opposite in comparison to the auto-peak at 1664 cm^{-1}.

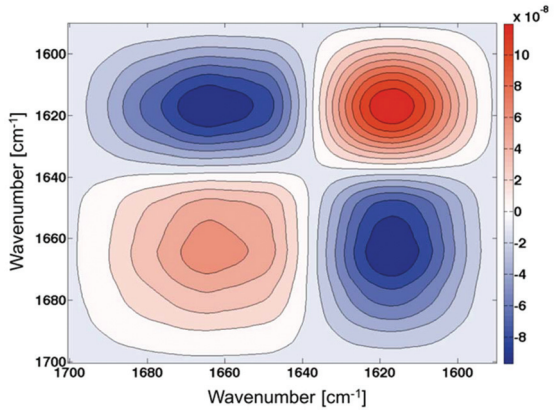

Fig. 3 Synchronous 2D correlation spectrum of human menisci during progressing degeneration.

In the asynchronous 2D correlation spectrum (Fig. 4), there is a total of four cross-peaks evident, *i.e.*, at 1674/1608, 1672/1648, 1647/1619, and 1629/1608 cm^{-1}. In the present study, the external perturbation is in fact the degeneration grade of the human menisci sample. Hence, the term 'sequential order' herein reflects the degree of change of the associated protein structures during meniscus degeneration, rather than a temporal change/perturbation. According to Noda's rules, the four cross-peaks therefore reveal the degree of total protein change as 1674 cm^{-1} > 1608 cm^{-1}, 1672 cm^{-1} > 1648 cm^{-1}, 1619 cm^{-1} > 1647 cm^{-1}, and 1629 cm^{-1} > 1608 cm^{-1}. Consequently, it is hypothesized that the spectral changes around the region 1619–1629 cm^{-1} and 1673 cm^{-1} region are stronger compared to the changes in the 1608 cm^{-1} and 1647 cm^{-1} regions during progressing degeneration. If compared with IR spectra of protein secondary structures, the 2D correlation spectra indicate that the side chains and the random structure of proteins in human menisci remain invariant or just slightly changed, while the content in triple helices and α-like helices appears significantly involved in meniscal degeneration during disease progression.

Discussion

Structural changes of collagen fibrils during meniscus degeneration

Collagen constitutes approx. 75% of the total meniscal tissue dry weight,[1] and is arranged in three distinct layers within the meniscus cross-section.[7] Due to the overwhelming presence and compact structure of collagen fibrils within the meniscus, as well as the maintained content in dry weight after degeneration[22] the majority of the features observed in the IR spectra may be attributed to collagen.

The collagen fibril structure is composed of three polypeptide chains, with each chain comprised of a $(Gly\text{-}X\text{-}Y)_n$ sequence as a left-handed α-like helix, in which proline and hydroxyproline are usually located at the X and Y position,

respectively. Three such α-like helices represent a polypeptide organized into a right-handed triple helix, which established the basic structure of collagen.[23–26] Furthermore, Lazarev *et al.* described that the amide I band of a triple-helical model spectrum includes three components. For example, the amide I band of the triple helix $(Gly\text{-}Pro\text{-}Pro)_n$ consists of three sub-peaks with their maxima at 1628 cm^{-1}, 1644 cm^{-1}, and 1664 cm^{-1}, which contribute to three stretching vibrations of two imine carbonyl and one amine carbonyl group in that order.[27] Upon dehydration of the triple-helical polytripeptide or *via* substitution of the solvent, a blue shift (*i.e.*, of the three sub-peaks at 1640 cm^{-1}, 1665 cm^{-1} and 1693 cm^{-1}) is observed. This results from the first imine carbonyl and the third amine carbonyl group changing to a quasi-free state due to the dissociated hydrogen–solvent bond. As a consequence, the order of the helix increases, while the molecular radius decreases.[27] In the current study, the most significant change during meniscus degeneration occurs as a distinct blue shift of the amide I band (*i.e.*, two area changes around 1624 cm^{-1} and 1664 cm^{-1}; Fig. 1, 3 and 4). As all lyophilized menisci samples were analysed at similar humidity, it is evident that the degeneration process negatively affects the hydrogen bond network between collagen and environmental water. Consequently, a decrease of the collagen molecular radius occurs thereby extending the triple-helical structure. Furthermore, for the samples in group grade 4 with calcification a maximum of the blue shift and area change of the amide I band was observed (Fig. 1). Hoshi *et al.* described in their study that physiological calcification causes removal of decorin (*i.e.*, a type of GAG), and fusion of collagen fibrils. This decreases the water-binding proteoglycan content within the collagen network, and increases the density of collagen fibrils.[28] If similar pathological mineralization occurs in soft tissue such as articular cartilage, this calcification could induce the degradation of the proteoglycan-collagen network, as well as cartilage deterioration.[29]

In summary, the blue shift and peak shape change of the amide I band during meniscus degeneration apparently includes distinct information on structural changes of collagen fibrils, their conformation, and a potential degradation of the water-binding proteoglycan-collagen network, especially if degenerated menisci are additionally calcified.

Changes in collagen and proteoglycan during meniscus degeneration

Proteoglycans represent the majority of organic matter in the extra cellular matrix (ECM), and are glycosylated molecules comprised of a core protein decorated with glycosaminoglycans (GAGs). Several kinds of GAGs are found in normal meniscus material, among which chondroitin-6-sulfate (CS6) amounts to approx. 60% of total GAGs. The main functions of proteoglycans are water absorption, network formation along with collagen fibrils, and the maintaining the tenacity of the meniscus tissue.[30] In addition, proteoglycan also plays an important role during collagen fibril maturation from procollagen, and during pathological mineralization.[28,29] Resulting, the content/percentage of proteoglycan is vital to the structural integrity of meniscus material, and to the network of collagen fibrils. Therefore, spectroscopically analysing proteoglycan may provide an additional indicator reflecting the condition of menisci.

As shown in the study of Pauli, during the degeneration of human menisci the GAG content increases significantly, as revealed by increasing safranin–O binding to negatively charged GAGs. A potential explanation for this increase could be a shift from a fibroblastic to a chondrocytic phenotype during early degeneration, as well as an accumulation of water-binding proteoglycans in degenerating human menisci.[5] An increase in safranin–O binding was indeed IR-spectroscopically observed in the present study, and used as a parameter for grading the degeneration progress *via* the obtained IR spectra.

In order to verify the validity of this concept, thus obtained grades were compared to the results of conventional histological staining, as shown in Fig. 5 illustrating the 2D correlation spectra of the collagen–chondroitin sulphate mixture model with changes of the ratio within the mixture serving as the external perturbation. The most significant change in the mixture model is the decrease in the 1625 cm^{-1} region, where

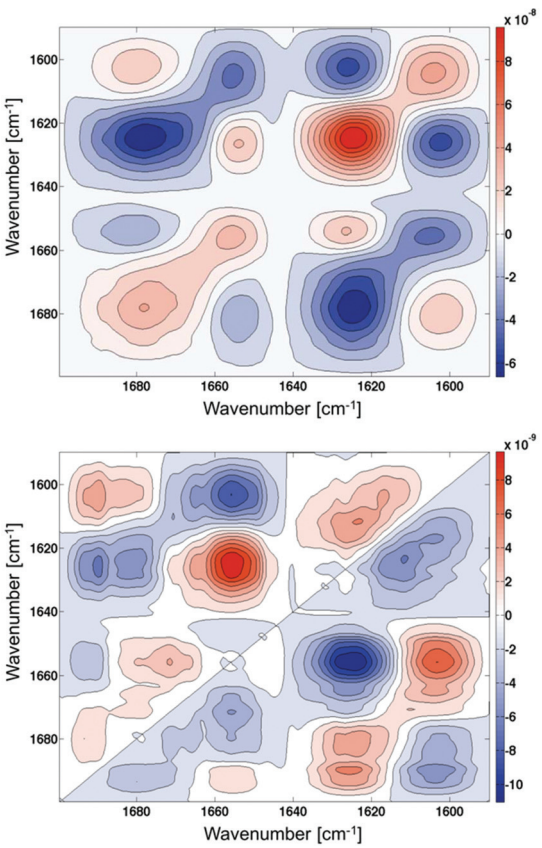

Fig. 5 Synchronous and asynchronous 2D correlation spectra of an artificial collagen–chondroitin sulphate mixture model. The chondroitin sulphate content percentage is raised from 4% to 41.2% serving as quasi-external perturbation.

the auto-peak has the highest value in the synchronous 2D correlation spectrum.

In contrast to the synthetically prepared mixture model, this change at 1625 cm^{-1} is overlapped in the entire regime by the auto-peak at 1617 cm^{-1} in the synchronous 2D correlation spectrum of human menisci samples (Fig. 3). Hence, it is hypothesized that indeed the change in proteoglycan content may contribute in part to the evident amide I band shape changes in the IR spectra of the human meniscus samples. As expected, there is no evident shift during any content change in the mixture model, and both characteristic peaks of collagen (*i.e.*, around 1630 cm^{-1} and 1653 cm^{-1}) decrease in the same direction. Also, in the asynchronous 2D correlation spectrum of the mixture model (Fig. 5), the very same cross-peak distribution is observed, but the order of change is opposite *vs.* the increasingly degenerated menisci spectra shown in the synchronous spectrum. Hence, the blue shift of the amide I band in the human meniscus samples with increasing degeneration mainly reveals the structural changes of the collagen fibrils. The content change in proteoglycan contributes partly to the amide I band shape changes in the region around 1625 cm^{-1}.

In summary, the IR spectra of human menisci provide molecular insight into structural changes of diseased cartilage at different degrees of degeneration derived from the amide I band, which combines content and structure variations of collagen fibrils and proteoglycan, as well as their network interaction. Most importantly, this information may potentially facilitate attributing the degree of degeneration following Pauli in future *via* label-free IR-diagnostic techniques. However, a more detailed contribution of each component to the amide I band is certainly required based upon the fundamental observations reported herein.

Conclusions

The present study illustrates that IR-ATR spectroscopy is a useful tool providing insight into molecular and structural changes of diseased cartilage during meniscus degeneration processes, and may be applied as a label-free diagnostic technique applied to the cartilage surfaces. One advantage of IR spectroscopy in comparison to the histological analysis for example is the potential objectifiability of the degeneration. 61 lyophilized human menisci samples at different states of degeneration were analysed during this study including grade 1 to grade 4 degeneration in part with calcification. A distinct blue shift of the amide I band (1700–1600 cm^{-1}) within meniscal IR-ATR spectra was observed, as well as significant variations in sub-peak areas representing secondary structure elements of the involved proteins *via* Gaussian fitting and peak deconvolution procedures separating degradation states grade 1, grade 4, and grade 4 with calcification.

Concerning the protein secondary structure information contained within the amide I band and the triple-helical structure of meniscal collagen, the observed blue shift and peak area changes of the amide I band are apparently associated with conformational changes of the collagen fibril structure during progressing degeneration, and the deterioration of the water-binding proteoglycan-collagen network. This is again and expectedly most pronounced for degenerated menisci with additional calcification.

2D correlation spectra using disease-associated changes (*i.e.*, progression from grade 1 to 4 in human meniscus samples or an increase in chondroitin sulphate in artificial mixtures with collagen) as quasi-external perturbation, additionally revealed that the changes in the amide I band are mainly associated with changes of the triple-helix and α-like helix structure of meniscal collagen during the degeneration process.

Herein the main changes observed have been based just on structural changes in collagen and proteoglycans, focusing on the spectral region 1700–1600 cm^{-1}. Nevertheless, other spectral regions, *e.g.* amide II band, C–H bending and sugar bands, can be analyzed in the future to evaluate the information provided by them.

In the current study, the low signal intensity and associated background noise when analysing lyophilized samples still limited a more pronounced analysis of the obtained results. Also, it should be pointed out that the ATR-IR spectrometer provide a limited sensitivity, nevertheless it was selected due to its portability, low cost and easy operation. Even at such conditions, ATR-IR has proven to be at useful tool for investigating human menisci degeneration. Hence, future studies will focus on optimizing the signal-to-noise ratio ideally working with fresh samples for providing even more distinctive information and label-free classification of the degree of cartilage degeneration information. Last but not least, current studies on developing IR-ATR technology into an *in vivo* applicable screening tool may potentially facilitate early degeneration detection without the requirement of collecting a sample from the patient.[31–37]

Conflicts of interest

There are no conflicts to declare.

Acknowledgements

PW is grateful for a graduate student fellowship provided by the International Graduate School in Molecular Medicine at Ulm University. This study is in part supported by the H2020-ICT-2016–2017 project MIRACLE (#780598) funded by the European Union.

References

1 H. Pereira, J. Silva-Correia, J. M. Oliveira, R. L. Reis and J. Espregueira-Mendes, in *Meniscal Transplantation*, Springer, Berlin, Heidelberg, 2013, pp. 7–14.

2 A. J. S. Fox, F. Wanivenhaus, A. J. Burge, R. F. Warren and S. A. Rodeo, *Clin. Anat.*, 2014, **28**, 269–287.
3 T. Brindle, J. Nyland and D. L. Johnson, *J. Athl. Train.*, 2001, **36**, 160–169.
4 R. Howell, *World J. Oncol.*, 2014, **5**, 597.
5 C. Pauli, S. P. Grogan, S. Patil, S. Otsuki, A. Hasegawa, J. Koziol, M. K. Lotz and D. D. D'Lima, *Osteoarthritis Cartilage*, 2011, **19**, 1132–1141.
6 E. A. Makris, P. Hadidi and K. A. Athanasiou, *Biomaterials*, 2011, **32**, 7411–7431.
7 W. Petersen and B. Tillmann, *Anat. Embryol.*, 1998, **197**, 317–324.
8 J. Herwig, E. Egner and E. Buddecke, *Ann. Rheum. Dis.*, 1984, **43**, 635–640.
9 M. Jakobs, V. Krenn, P. Knoess, B. Kurz and M. Otto, *J. Orthop. Traumatol.*, 2011, **1**, 1–7.
10 P. A. West, M. P. G. Bostrom, P. A. Torzilli and N. P. Camacho, *Appl. Spectrosc.*, 2004, **58**, 376–381.
11 N. P. Camacho, P. West, P. A. Torzilli and R. Mendelsohn, *Biopolymers*, 2001, **62**, 1–8.
12 M. Jackson and H. H. Mantsch, *Crit. Rev. Biochem. Mol. Biol.*, 1995, **30**, 95–120.
13 H. H. Mantsch and D. Chapman, *Infrared Spectroscopy of Biomolecules*, John Wiley & Sons, New York, 1996.
14 A. Barth, *Biochim. Biophys. Acta, Bioenerg.*, 2007, **1767**, 1073–1101.
15 E. Goormaghtigh, J.-M. Ruysschaert and V. Raussens, *Biophys. J.*, 2006, **90**, 2946–2957.
16 A. Boskey and N. Pleshko Camacho, *Biomaterials*, 2007, **28**, 2465–2478.
17 K. Belbachir, R. Noreen, G. Gouspillou and C. Petibois, *Anal. Bioanal. Chem.*, 2009, **395**, 829–837.
18 A. Hanifi, H. McCarthy, S. Roberts and N. Pleshko, *PLoS One*, 2013, **8**, e64822.
19 M. Son, S. B. Goodman, W. Chen, B. A. Hargreaves, G. E. Gold and M. E. Levenston, *Osteoarthritis Cartilage*, 2013, **21**, 796–805.
20 A. M. Seitz, F. Galbusera, C. Krais, A. Ignatius and L. Dürselen, *J. Mech. Behav. Biomed. Mater.*, 2013, **26**, 68–80.
21 I. Noda and Y. Ozaki, *Two-dimensional correlation spectroscopy: applications in vibrational and optical spectroscopy*, John Wiley & Sons Ltd, 2005.
22 J. Herwig, E. Egner and E. Buddecke, *Ann. Rheum. Dis.*, 1984, **43**, 635–640.
23 K. Beck and B. Brodsky, *J. Struct. Biol.*, 1998, **122**, 17–29.
24 B. Brodsky and J. Ramshaw, *Matrix Biol.*, 1997, **15**, 545–554.
25 C. Petibois and G. Déléris, *Trends Biotechnol.*, 2006, **24**, 455–462.
26 M. D. Shoulders and R. T. Raines, *Annu. Rev. Biochem.*, 2009, **78**, 929–958.
27 Y. A. Lazarev, B. A. Grishkovsky and T. B. Khromova, *Biopolymers*, 1985, **24**, 1449–1478.
28 K. Hoshi, S. Kemmotsu, Y. Takeuchi, N. Amizuka and H. Ozawa, *J. Bone Miner. Res.*, 1999, **14**, 273–280.
29 T. Kirsch, *Curr. Opin. Rheumatol.*, 2006, **18**, 174–180.
30 E. A. Makris, P. Hadidi and K. A. Athanasiou, *Biomaterials*, 2011, **32**, 7411–7431.
31 L. Wang, J. Chapman, R. A. Palmer, T. Alter, B. Hooper, O. Van Ramm and B. Mizaikoff, *Appl. Spectrosc.*, 2006, **60**, 1121–1126.
32 L. Wang, J. Chapman, R. A. Palmer, O. Van Ramm and B. Mizaikoff, *J. Biomed. Opt.*, 2007, **12**, 0240061–0240011.
33 L. Wang and B. Mizaikoff, *Anal. Bioanal. Chem.*, 2008, **391**, 1641–1654.
34 P. Wang, W. Bohr, M. Otto, K. M. Danzer and B. Mizaikoff, *Anal. Bioanal. Chem.*, 2015, **407**, 4015–4021.
35 Á. I. López-Lorente, P. Wang, M. Sieger, E. V. Catalan, M. Karlsson, F. Nikolajeff, L. Österlund and B. Mizaikoff, *Phys. Status Solidi A*, 2016, **8**, 2117–2123.
36 Á. I. López-Lorente and B. Mizaikoff, *Anal. Bioanal. Chem.*, 2016, **408**, 2875–2889.
37 Á. I. López-Lorente, P. Wang and B. Mizaikoff, *Microchim. Acta*, 2017, **184**, 453–462.